reaching a maximum for $\mu = -45°$ and $\sin^2\theta = 0{\cdot}86$ of only 0·0015. Since this is in every respect an extreme case, errors due to crystal missetting may be safely ignored. This relative insensitivity to the value of $\mu$ also explains why the program converges rapidly in $a$.

The method is very insensitive to the camera radius. A change of 1% in the value used for the aenigmatite data produced only a change of 0·03% in the calculated unit-cell dimensions.

## Conclusions

This extension of Main & Woolfson's technique has the advantages that only data about a single axis are required, and that (even when data from several axes are available) more information can be incorporated. It can also be recommended as a quick and highly effective check that a set of upper-layer Weissenberg photographs have been consistently indexed, since an incorrectly indexed reflexion is immediately apparent on comparing the $\sin^2\theta$ values from the $\alpha$ doublet separations with those calculated from the analytical constants.

We are very grateful to Dr C.H.Kelsey and Dr D. McKie for their carefully measured data.

## References

ALCOCK, N. W. & RASPIN, K. A. (1967). To be published.
*International Tables for X-ray Crystallography* (1959). Vol.II, p.92 and 176. Birmingham: Kynoch Press.
KELSEY, C. H. & MCKIE, D. (1964). *Miner. Mag.* **33**, 986.
MCKIE, D. (1966). Personal communication.
MAIN, P. & WOOLFSON, M. M. (1963). *Acta Cryst.* **16**, 731.

*Acta Cryst.* (1967). **23**, 38

# Diffuse Double Diffraction of X-Rays

BY S. L. STRONG* AND ROY KAPLOW

*Department of Metallurgy, Massachusetts Institute of Technology, Cambridge, Massachusetts* 02139, *U.S.A.*

(*Received* 5 *May* 1966 *and in revised form* 31 *August* 1966)

A Monte Carlo method has been used to evaluate the magnitude of twice scattered X-rays in diffraction experiments. The quantitative effects of variations in the primary scattering distribution, the absorption coefficient, the scattering power of the atoms, the X-ray wavelength, the specimen thickness, the monochromator and slit configuration and of polarization corrections have been derived. These factors have various influences on the magnitude and angular distribution of the twice scattered radiation but $I_2(\theta)$ is of the order of 0·0025 $\sigma^2/\mu_p W$ (electron units per atom) for all the elements and conditions considered, where $\sigma^2$ is the square of the primary diffraction cross-section, $\mu$ is the mass absorption coefficient and $W$ is the atomic weight.

The experimental measurements of diffusely scattered radiation include contributions due to multiply scattered radiation. Often, this contribution must be accounted for in order to analyse the coherently diffracted component. Chandrasekhar (1950) has derived certain expressions for the multiple scattering of radiation but these are not directly applicable to most diffraction experiments. Vineyard (1954) has obtained expressions for the doubly scattered component of neutron radiation, with isotropic primary scattering $[I_1(\theta)]$ and two common diffraction geometries. Warren (1959*a*) has obtained numerical values for the double scattering of Cu $K\alpha$ X-radiation from a polycrystalline sample of copper in the normal Bragg–Brentano X-ray reflection geometry, representing the primary scattering as a finite sum of sharp reflections. The conditions assumed in either of these two calculations would not appear to be applicable to liquid or amorphous specimens. With such materials $I_1(\theta)$ is not isotropic nor does it consist of a few sharp reflections. In addition, if absorption in the sample is low, and if the incident and detected beams are restricted (as they are by slits or monochromators) the geometrical conditions may be abnormal.

In this paper we present the results of more general Monto Carlo calculations. The quantitative effects on the double scattering of variations in the primary scattering distribution, the absorption coefficient, the scattering power of the atoms, the specimen thickness, the monochromator configuration and of polarization corrections are shown. We consider only the double scattering of X-rays from the 'surface' of a flat sample large enough to intercept the entire beam, with source and detector situated symmetrically with respect to the surface normal.

* Present address, Union Carbide Corp., Cleveland, Ohio, U.S.A.

## Analysis

The path of a detected ray which is scattered twice in a flat sample of constant thickness, $t$, but of effectively infinite extent in the $x$ and $y$ directions is shown in Fig. 1. The incident and emergent rays are constrained to lie in parallel planes which are normal to the specimen surface, and both rays are at the angle $\theta$ with respect to the specimen surface. These conditions imply that angular divergences in both the incident and detected beams are ignored. The first scattering, by angle $\xi_1$, occurs in volume element $dv_1$ a distance $l_1$ from the point of entry; the second scattering, by angle $\xi_2$, occurs in volume element $dv_2$, a distance $l_2$ from the first scattering point; the ray emerges at point $x_0, y_0$, a distance $l_3$ from the second scattering point.

The differential of the absolute twice diffracted intensity, $\delta[I_2^a(\theta)]$, from the volumes $dv_1$ and $dv_2$ is

$$\delta[I_2^a(\theta)] = I_0 K^2 I_1(\xi_1/2) I_1(\xi_2/2) P(\xi_1,\xi_2,\theta,\theta_M) \times \frac{\exp(-\mu l_1)\exp(-\mu l_2)\exp(-\mu l_3)}{(l_2)^2 R^2} dv_1 dv_2 , \quad (1)$$

where:

$I_0$ = incident beam intensity
$K = \varrho e^4/m_0^2 c^4$
$\varrho$ = density (atoms cm$^{-3}$)
$P(\xi_1,\xi_2,\theta,\theta_M)$ = polarization factor (see Appendix); $\theta_M$ is the monochromator Bragg diffraction angle.

$R$ = radius of receiving surface
$\mu$ = linear absorption coefficient
$I_1$ = primary scattering intensity (electron units per atom; see below).

The relationship between absolute units and electron units per atom (eu.a$^{-1}$), which are usually more convenient to use, is:

$$I^a(\theta) = I(\theta) I_0 A G(\theta) K P(\theta)/2\mu R^2 , \quad (2)$$

where

$I^a(\theta)$ = intensity in absolute units
$I(\theta)$ = intensity in eu.a$^{-1}$
$A$ = area of incident beam
$G(\theta)$ = factor to correct for the finite sample thickness or the limitations of the diffraction geometry.

$P(\theta)$ = single scattering polarization factor (see Appendix).

The twice-scattered intensity is obtained by integrating over the entire irradiated volume and along the path $l_3$ and averaging over the surface area as seen by the detector. In electron units,

$$I_2(\theta) = \frac{2K\mu}{I_0 PG} \Big\langle \int^{t/\sin\Theta} dl_3 \exp(-\mu l_3) \iiint_{\text{irradiated volume}} dx_1 dy_1 dz_1 I(\xi_1/2) I(\xi_2/2) P(\xi_1,\xi_2,\theta,\theta_M) \frac{\exp(-\mu l_1)\exp(-\mu l_2)}{(l_2)^2} \Big\rangle_{\text{averaged over } x_0\, y_0} \quad (3)$$

where $t$ is the thickness of the sample.

The direct analytical solution of the sixfold integral in equation (3) is possible only for severely restrictive conditions. Numerical integration is feasible, in principle, with a high speed computer, but difficulties regarding the choice of an appropriate mesh and the specification of the integration boundaries in all but the simplest cases make such a procedure disadvantageous. Our evaluation of equation (3) is based on the fact that the value of any integral is equal to the average value of the integrand in the volume of integration, multiplied by the volume:

$$\int U dv = V_0 \langle U \rangle_{V_0} .$$

The average value of the integrand

$$I(\xi_1/2) I(\xi_2/2) P(\xi_1,\xi_2,\theta,\theta_M) \times \exp(-\mu l_1)\exp(-\mu l_2)\exp(-\mu l_3)/(l_2)^2 \quad (4)$$

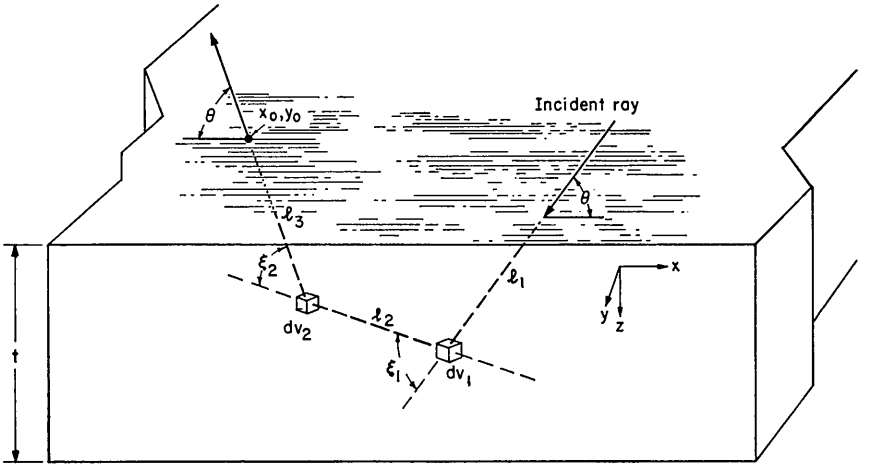


Fig. 1. Double scattering geometry, in three dimensions.

is computed with a statistically meaningful number of sets of random values of the variables of integration. (In the computer calculations it is actually most convenient to use $\theta, l_3, x_0, y_0$ and the location of the first scattering volume, $x_1, y_1, z_1$ as the independent variables). This average, multiplied by the numerical factor $2K\mu V_0/I_0AG$, is the magnitude of the twice scattered radiation.

Such a procedure is directly analogous to the random nature of the scattering process itself, and the precision of the result is limited only by the number of samples included. In order to enhance the convergence, we have used a number of standard Monte Carlo devices, such as Russian roulette, weighted sampling, and analytical averaging (Meyer, 1956). For all the results presented here, for example, the variables $l_3$ and $z_1$ have been preferentially weighted towards values that make the largest contributions to the intensity. The values for these variables have been based on the square of a random number (between 0·0 and 1·0) rather than on the random number itself, and the resulting contribution to the intensity has been divided by the relative probability of the occurrence of those particular values. For most geometries, weighted sampling could be utilized for other variables as well. The most significant improvement in the calculation speed, however, is obtained by replacing the term

$$\exp(-\mu l_1)\exp(-\mu l_2)\exp(-\mu l_3)/(l_2)^2 \qquad (5)$$

by an analytical average whenever $l_2$ is less than a particular small value, $R_m$. Term (5) is replaced by $C\exp(-2\mu l_3)$, where $C$ is the value of $[\exp(-\mu[l_1-l_3])\exp(-\mu l_2)]/(l_2)^2$, averaged over a small sphere of radius $R_m$, centered at the second scattering volume:

$$C=\frac{1}{\frac{4}{3}\pi R_m^3}\int_0^{2\pi}d\varphi\int_0^{\pi}d\theta\int_0^{R_m}\frac{r^2\sin\theta\exp\{-r(1-\cos\theta/\sin\theta)\}}{r^2}dr\,. \qquad (6)$$

$\theta$, $\varphi$ and $r$ describe the position of the first scattering volume, relative to the second. The integral can be expressed by the series:

$$C=\frac{3}{2}\frac{\sin\theta}{R_m^3\mu}\sum_{n=1}^{\infty}\frac{[(1-\csc\theta)^n-(1+\csc\theta)^n](-\mu R_m)^n}{n\,.\,n!}\,. \qquad (7)$$

The error caused by the approximation of this substitution is slight as long as $R_m$ is chosen to be significantly less than an absorption length ($1/\mu$). For most of the results presented here the substitution was made whenever $l_2$ was less than $1/10\mu$, which causes a negligible error. ( A less conservative value could have been used, since $R_m=\frac{1}{2}\mu$ allows an additional tenfold reduction in computation time, with an error of less than 4%).

The double scattering values presented, in the next section, each represent 30,000 to 100,000 random choices of variables and are estimated to be within ±5% of the exact values. This significance required 1 to 2 minutes for each value of $\theta$ (10–20 minutes for each curve of 10 points) on the M.I.T. Computation Center IBM 7094 computer.

## Results

An $I_2'(\theta)$ may be defined, which is independent of the average scattering power and of the absorption coefficient, and for which dimensions may be expressed relative to the linear absorption coefficient:

$$I_2'(\theta)=I_2(\theta)\mu m_0^2c^4/\sigma^2\varrho e^4=I_2(\theta)\mu_\varrho W/0{\cdot}048\sigma^2\,, \qquad (8)$$

where

$\mu_\varrho$ = mass absorption coefficient

$$\sigma=2\pi\int_0^{\pi}I_1(2\theta)\sin 2\theta\,d(2\theta)$$

$W$ = atomic weight.

Our calculations show that $I_2'(\theta)$ is of the order of 0·02 for all of the conditions considered. Therefore, the average level of the multiple scattering depends primarily on the properties $\sigma$, $W$ and $\mu_\varrho$. The actual distribution, however, is affected by the primary scattering and by other details of the experiment.

The constant $\sigma$, which is a measure of the total scattering cross section, varies with atomic number, $Z$, the wavelength of the radiation and the shape of $I_1(\theta)$. Fig. 2 shows the variation for $Z=5$ through 30 with both Cu $K\alpha$ and Mo $K\alpha$ radiations and $I_1(\theta)=ff^*$. $\sigma$ is roughly proportional to $Z^2$, except in the neighborhood of absorption edges. Structure-dependent diffraction effects in liquid and amorphous materials alter $I_1(\theta)$ and may thereby modify $\sigma$ by 10–20%, so the values in Fig. 2 should not be used indiscriminately.

In Fig. 3 we compare the results of Vineyard's analytical calculation with a Monte Carlo analysis which simulates Vineyard's conditions of infinite boundaries, isotropic primary scattering and no polarization effects. In X-ray experiments the measured intensity is

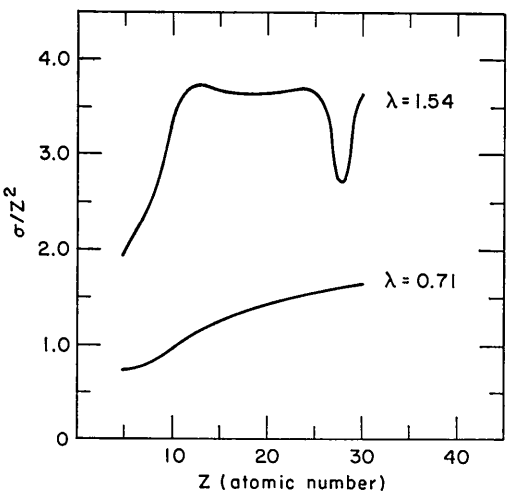


Fig. 2. Variation of the total scattering cross-section per atom with atomic number and X-ray wavelength.

usually converted to electron units (or some multiple thereof) by dividing the measured values by the polarization function appropriate to single scattering. In Fig. 3 we also show the effect of the true polarization on $I_2'(\theta)$ (with no monochromators) and the extent to which the normal polarization correction accounts for the polarization effect. The overall result of polarization effects in the scattering processes, combined with the normal 'correction', is to reduce the multiple scattering by about 30%. In each of the subsequent figures, $I_2'(\theta)$, has been divided by the appropriate single scattering X-ray polarization correction, since that is the form in which data are normally examined.

Warren's polycrystalline calculation for copper is at the extreme opposite from the assumption of isotropic scatters. In Fig. 4 we compare that result with a Monte Carlo calculation with $I_1(\theta)$ equal to $f^2 + I_{\text{Compton modified}}$ (to match Warren's values). The peaks in Warren's result, in particular the peak at the origin, are due to the presence of the sharp, intense peaks in the crystalline $I_1(\theta)$. Beyond $2\theta = 20°$, however, the independent scattering result is remarkably similar. In Fig. 5, three $I_2'(\theta)$ are shown, which have been calculated for (*a*) independent scattering ($I_1(\theta) = ff^*$) and [(*b*) and (*c*)] for two pseudo-liquid primary scattering functions, both based on the same scattering factors.

These comparisons show that the multiple scattering is affected very little by the details in the primary scattering as long as $I_1(\theta)$ represents a reasonable sampling of $ff^*$. Therefore, Vineyard's 'isotropic' calculation should be a good approximation even for polycrystalline samples with neutron radiation, except at low angles, as has been demonstrated experimentally (Blech & Averbach, 1965).

Calculations have also been made to investigate the effect of such systematic variations in $I_1(\theta)$ as arise from the variation of $ff^*/\sigma$ with $Z$ and the changes in shape encountered with different values of X-ray wavelength for a given $Z$. The results of these calculations are shown in Figs. 6 and 7. One finds that for $2\theta$ less than 90°, $I_2'(\theta)$ follows the trends in $I_1(\theta)$ while in the high angle region $I_2'(\theta)$ is practically independent of the shape of the primary scattering. Finally, in Figs. 8 and 9, we illustrate the effects of monochromators, finite sample thickness and finite diffraction geometry. With the latter two of these, the measured single scattered intensity requires corrections (Milberg, 1958) in

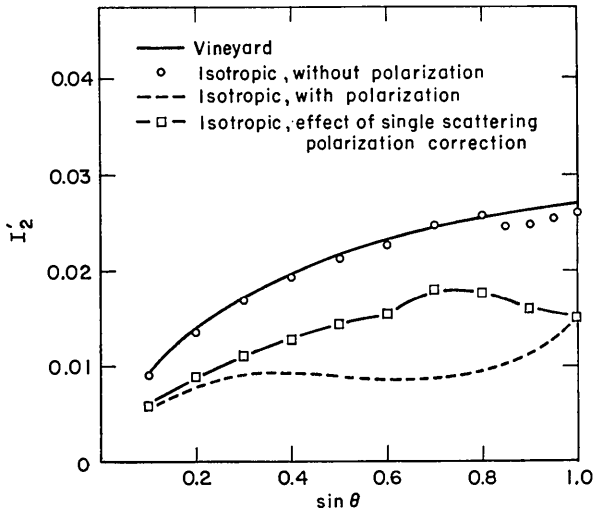


Fig. 3. Double scattering with isotropic primary scattering. Effects of polarization and standard polarization correction.

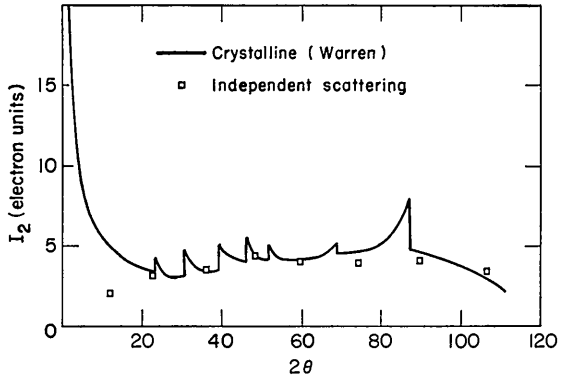


Fig. 4. Comparison of double scattering with discrete peak and independent primary scattering (copper with Cu $K\alpha$ radiation).

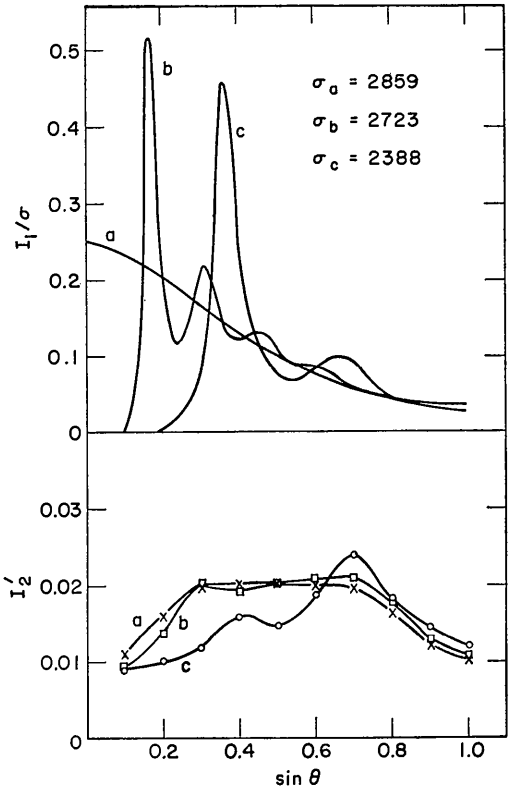


Fig. 5. Comparison of double scattering with three different primary scattering distributions. (*a*) Independent scattering. (*b*) and (*c*) Pseudo-liquids.

addition to the polarization function, and these have also been applied to $I_1'(\theta)$. The sample thickness has little effect on $I_2'(\theta)$, but restrictive geometry ($0{\cdot}5/\mu$ incident beam width, $1{\cdot}5/\mu$ receiver acceptance) reduces the double scattering appreciably. The effect of monochromators, which is to reduce the double scattering, as illustrated in Fig. 9, is due to the depolarization of the beam by the multiple scattering processes. The latter calculations apply to Cu $K\alpha$ radiation and LiF monochromators.

## Discussion

The mathematical technique employed for these calculations is not limited to X-ray diffraction or to the particular sample configuration which we have discussed. The method is quite generally applicable, provided that one is not interested in the low angle region when sharp, intense reflections are present (Warren, 1959*b*).

From the data presented here it should be possible to estimate the magnitude and shape of the multiple scattering for any experiment with a geometry comparable to that which we have considered. In this regard, it should be noted, in considering the shape of $I_1(\theta)$ and the value of $\sigma^2$, that the incoherent contribution to the primary scattering may not be negligible for the lighter elements, if it is not eliminated experimentally. As a general rule-of-thumb, $I_2(\theta)_{\text{eua}-1}$ is less than $0{\cdot}005\ \sigma^2/\mu_e W$ and is likely to be of the order of $0{\cdot}001\sigma^2/\mu_e W$.

This work was sponsored in part by the Office of Naval Research, under Contract Nonr-1841(48). All of the computer calculations were done at the M.I.T. Computation Center. We also appreciate the continuing interest and advice of Professor B. L. Averbach.

## APPENDIX

*Polarization factors*

The polarization factor for single scattering, in the absence of crystal monochromators, with initially unpolarized radiation is (James, 1962):

$$P(\theta)=\frac{1+\cos^2 2\theta}{2}. \qquad (A1)$$

With, respectively, one and two (identical) crystal monochromators in the diffractometer system, the polarization factors for single scattering are (Cullity, 1956):

$$P(\theta)=\frac{1+\cos^2 2\theta\,\cos^2 2\theta_M}{2} \qquad (A2)$$

and

$$P(\theta)=\frac{1+\cos^2 2\theta\,\cos^4 2\theta_M}{2}. \qquad (A3)$$

Warren (1959*a*) has given the polarization factor for double diffraction without monochromators:

$$P(\xi_1,\xi_2,\theta)=[\cos^2\xi_1+\cos^2\xi_2+ +(\cos 2\theta-\cos\xi_1\cos\xi_2)^2]/2\,. \qquad (A4)$$

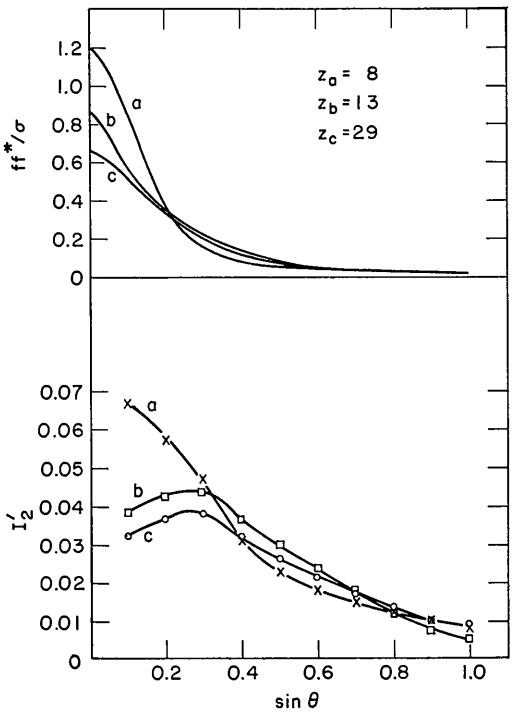


Fig. 6. Variation of double scattering with atomic number of scatterer.

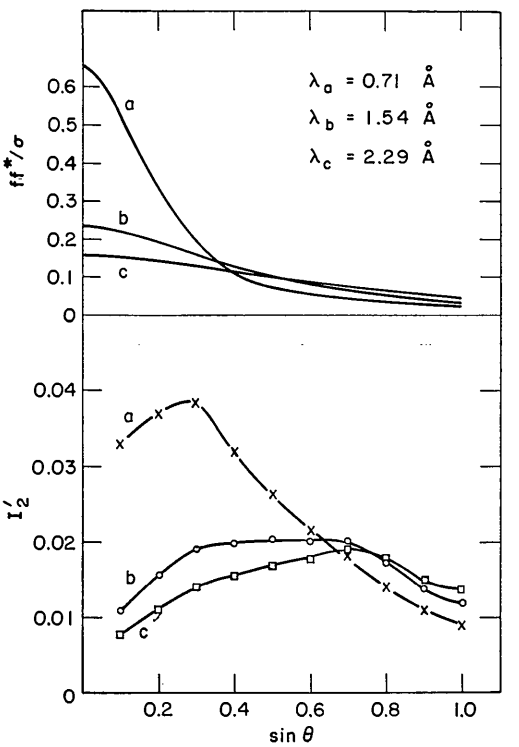


Fig. 7. Variation of double scattering with X-ray wavelength.

The calculation may be extended to a diffraction geometry which includes monochromators in the incident and/or diffracted beams. The spherical triangle formed by the angles $\xi_1$, $\xi_2$, and $2\theta$ in Fig. 10 is a helpful construction for this purpose. The three angles and the diffraction geometry at the specimen have been defined in the previous text with respect to Fig. 1. The monochromators operate in planes parallel to the 'plane' of diffraction at the specimen.

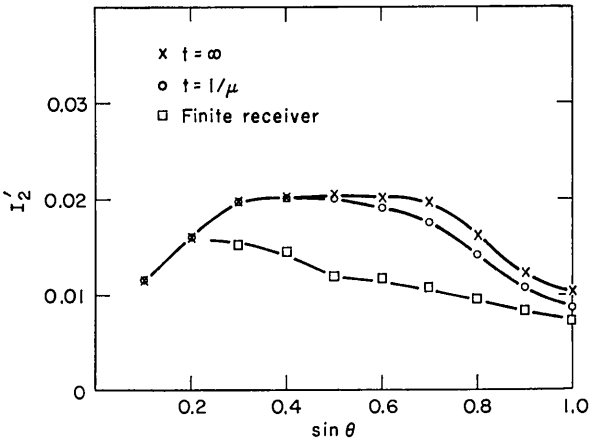


Fig. 8. The effects of finite thickness ($t = 1/\mu$) and finite geometry (incident beam width = $0{\cdot}5/\mu$, receiver acceptance = $1{\cdot}5/\mu$).

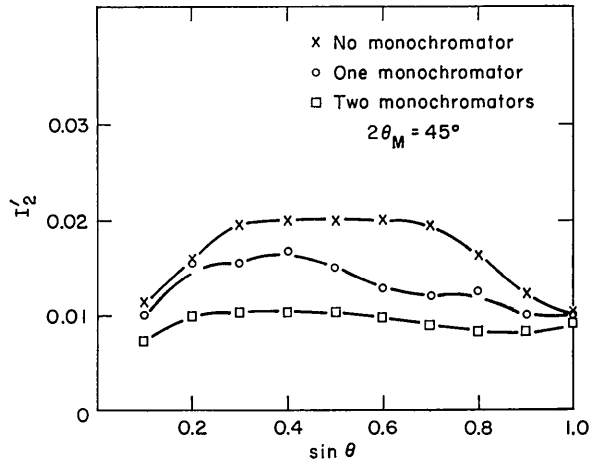


Fig. 9. The effects of monochromators (LiF crystals and Cu $K\alpha$ radiation).

The spherical triangle, on a sphere much larger than the specimen, is defined by points $X, Y, Z$ which are respectively the points at which the incident, once-diffracted and twice-diffracted rays would emerge from the sphere. The angles of the triangle may be expressed in terms of the diffraction angles:

$$\cos\varphi = \frac{\cos\xi_2 - \cos 2\theta \cos\xi_1}{\sin 2\theta \sin\xi_1}$$

$$\cos\chi = \frac{\cos 2\theta - \cos\xi_1 \cos\xi_2}{\sin\xi_1 \sin\xi_2}$$

$$\cos\gamma = \frac{\cos\xi_1 - \cos 2\theta \cos\xi_2}{\sin 2\theta \sin\xi_2}. \qquad (A5)$$

With an unpolarized source the relative components of the electric vectors of the radiation after the diffraction at the first monochromator are

$$E_\perp = 1/\sqrt{2}$$
$$E_\parallel = Q/\sqrt{2} \qquad (A6)$$

where $E_\perp$ and $E_\parallel$ are perpendicular and parallel, respectively, to the plane of diffraction of the monochromator and $Q = \cos 2\theta_M$.

After the first diffraction in the sample

$$E_\perp = \sqrt{Q^2 + \cos^2\varphi(1-Q^2)}/\sqrt{2}$$
$$E_\parallel = \cos\xi_1 \sqrt{1 + \cos^2\varphi(Q^2-1)}/\sqrt{2}, \qquad (A7)$$

where the direction subscripts now refer to the first diffraction plane, *i.e.* the plane defined by $l_1$ and $l_2$.

After the second diffraction in the sample

$$E_\perp = \{\cos^2\chi[Q^2 + \cos^2\varphi(1-Q^2)] + \sin^2\chi \cos^2\xi_1[1 + \cos^2\varphi(Q^2-1)]\}^{\frac{1}{2}}/\sqrt{2}$$

$$E_\parallel = \cos\xi_2\{\sin^2\chi[Q^2 + \cos^2\varphi(1-Q^2)] + \cos^2\chi \cos^2\xi_1[1 + \cos^2\varphi(Q^2-1)]\}^{\frac{1}{2}}/\sqrt{2}, \qquad (A8)$$

where the direction subscripts refer to the second diffraction plane, *i.e.* that defined by $l_2$ and $l_3$. The po-

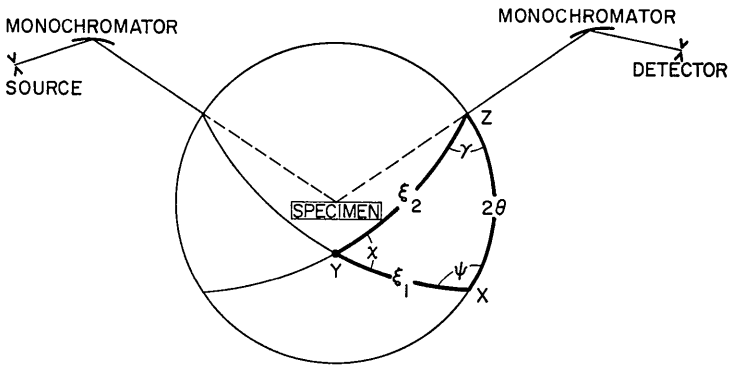


Fig. 10. Construction for the calculation of polarization factors.

larization factor for double diffraction with one monochromator is therefore:

$$P(\xi_1,\xi_2,\theta,\theta_M)=\{Q(\cos^2\chi+\sin^2\chi\,\cos^2\xi_2)+\cos^2\xi_1(\sin^2\chi+\cos^2\chi\,\cos^2\xi_2)+(1-Q)\cos^2\varphi(\cos^2\chi\,\sin^2\chi\,\cos^2\xi_1-\sin^2\chi\,\cos^2\xi_2-\cos^2\chi\,\cos^2\xi_1\,\cos^2\xi_2)\}/2\,. \quad (A9)$$

Including the effect of the second monochromator yields:

$$P(\xi_1,\xi_2,\theta,\theta_M)=[D\{\cos^2\gamma\,\cos^2\chi+\sin^2\gamma\,\sin^2\chi\,\cos^2\xi_2\}+B[\cos^2\gamma\,\sin^2\chi\,\cos^2\xi_1+\sin^2\gamma\,\cos^2\chi\,\cos^2\xi_1\,\cos^2\xi_2]+Q\{D[\sin^2\gamma\,\cos^2\chi+\cos^2\gamma\,\sin^2\chi\,\cos^2\xi_2]+B[\sin^2\gamma\,\sin^2\chi\,\cos^2\xi_1+\cos^2\chi\,\cos^2\gamma\,\cos^2\xi_1\,\cos^2\xi_2]\}]/2 \quad (A10)$$

where:

$$D=Q+(1-Q)\cos^2\varphi$$
$$B=1-(1-Q)\cos^2\varphi\,.$$

### References


BLECH, I. A. & AVERBACH, B. L. (1965). *Phys. Rev.* **137A**, 1113.

CHANDRASEKHAR, S. (1950). *Radiation Transfer*, Chapter IX. Oxford: Clarendon Press.

CULLITY, B. D. (1956). *Elements of X-Ray Diffraction*, p.172. Reading, Mass.: Addison-Wesley.

JAMES, R. W. (1962). *The Optical Principles of the Diffraction of X-Rays*, p.31. London: Bell.

MEYER, H. A. (1956). *Symposium on Monte Carlo Methods*. New York: John Wiley.

MILBERG, M. E. (1958). *J. Appl. Phys.* **29**, 64.

VINEYARD, G. H. (1954). *Phys. Rev.* **96**, 93.

WARREN, B. E. (1959*a*). *J. Appl. Phys.* **30**, 111.

WARREN, B. E. (1959*b*). *Acta Cryst.* **12**, 837.


*Acta Cryst.* (1966). **23**, 44

# Theory of X-Ray Diffraction In Crystals With Stacking Faults


BY W. H. ZACHARIASEN

*Department of Physics, University of Chicago, Chicago, Illinois, U.S.A.*


(*Received* 28 *June* 1966)


X-ray diffraction in a crystal with stacking disorder is studied theoretically. It is assumed that the layers are identical and equidistant. If $\mathbf{a}_2$ is the stacking direction, diffraction occurs when the scattering vector $\mathbf{s}$ satisfies the condition $\mathbf{s}=2\pi[H_1\mathbf{b}_1+y\mathbf{b}_2+H_3\mathbf{b}_3]$, where $H_1, H_3$ are integers, but $y$ may have any value. As to intensity of scattering, the observable quantity is the integrated intensity $P_{H_1H_3}(y)$, and the detailed expression for this function is deduced. For an ordered crystal the integrated intensity is invariant under the symmetry operations of the crystal as applied to the indices $H_1H_2H_3$, but this is not true in general of $P_{H_1H_3}(y)$. Thus $P_{H_1H_3}(y)\neq P_{H_1H_3}(-y)$ when $\mathbf{b}_2$ is the normal to a mirror plane. It is shown how the precise nature of the stacking disorder can be deduced by means of a detailed analysis of the experimental curves $P_{H_1H_3}(y)$.


## Introduction

A structure study of a single crystal of $\beta$-$Ca(BO_2)_2$ was recently begun by the writer. The crystal is orthorhombic with periods $a_1=8{\cdot}369\pm0{\cdot}001$, $a_2=13{\cdot}816\pm0{\cdot}001$, $a_3=5{\cdot}007\pm0{\cdot}001$ Å; but the X-ray diffraction patterns are unusual. Diffraction occurs for integral values of the Miller indices $H_1$ and $H_3$, and when $H_3$ is even also for integral values of $H_2$. However, diffraction takes place for any value $y$ of the second index when $H_3$ is odd. In other words, the diffraction conditions are those of a three-dimensional lattice if $H_3$ is even, those of a two-dimensional lattice if $H_3$ is odd. The diffraction vectors $\mathbf{s}$ are thus of the form

$$H_3 \text{ even: } \mathbf{s}=2\pi[H_1\mathbf{b}_1+H_2\mathbf{b}_2+H_3\mathbf{b}_3]$$
$$H_3 \text{ odd: } \mathbf{s}=2\pi[H_1\mathbf{b}_1+y\mathbf{b}_2+H_3\mathbf{b}_3] \quad (1)$$

where $y$ may have any value.

Extensive integrated intensity measurements have been made for zones $[H_1yH_3]$ with $H_3$ odd, using both Cu $K\alpha$ radiation with a 'normal beam' counter spectrometer and Mo $K\alpha$ radiation with a 'goniostat' spectrometer. As an illustration Table 1 shows the measured values of the integrated intensity $P_{H_1H_3}(y)$ for the reciprocal lattice row $[2y1]$ at intervals of 0·1 for $y$ over the range $-9\leq y\leq+9$. Intensity maxima occur at integral and half-integral values of $y$, but about eighty per cent of the scattering is in the background between the maxima. The most remarkable feature of Table 1 is the experimental fact that the integrated intensities $P_{H_1H_3}(y)$ and $P_{H_1H_3}(\bar{y})$ are different. The symmetry of the crystal being centrosymmetric orthorhombic, one has $|F_{H_1H_3}(y)|=|F_{H_1H_3}(\bar{y})|$, and it is, therefore, startling to find that the integrated intensity is not invariant under the symmetry operations of the crystal.